Impulse Analysis of Isolated and Interconnected WTGSs under Lightning Discharges

O. Kherif, S. Chiheb, M. Teguar and A. Mekhaldi

Abstract—Most of the malfunctions of electrical systems inside wind turbine, including the control ones, are related to the ground potential rise of the grounding system resulting from lightning discharge. Indeed, the performance of such systems mainly depends on the lightning current wave propagation characteristics. Large grounding system performance against lightning discharge depends on the current wave propagation characteristics through the grounding system. It is in this light that the paper proposes to analyse and discuss the impulse behaviour of Wind Turbine Grounding System (WTGS). The interconnection effect on the lightning response of WTGS has been investigated for various values of soil resistivities. Also, the paper discusses the feed point effect for typical small wind farm. It is found that the soil resistivity has a significant influence affecting the transient response of WTGS while the interconnection facilitates the flow of the current into the ground. For interconnected systems, it is shown that the injection at the middle wind turbines gives the lower ground potential rise, thus, more suitable results than the other ones. It is suggested that the wind turbines of the middle should be more taller than the other, especially for those installed in areas characterizing by high values of soil resistivity.

Index Terms—Wind turbine, Grounding, Lightning protection, Transient response, Transmission line approach.

1 Introduction

NOWADAYS, wind turbines are considered as the most important source of renewable energy. Such energy systems, whose essential purpose is to ensure a continuous supply, must be equipped with powerful means of protection. The necessity of preinspections cannot be neglected, and a good design of the protection plan can protect individuals near such systems and minimize the undesirable outage, down-time and loss of revenue.

Practically, wind turbines with tall structures are installed across large areas characterising by highest wind density [1]. Their locations are suspected to be the target of lightning discharge, considered as the major threat which could cause significant damages [2]. Most of the malfunctions of the electrical and/or control systems inside wind turbines are caused by Ground Potential Rise (GPR) due to lightning discharge [3].Therefore, the WTGS should be adequately designed to avoid excessive voltage surges and excessive potential gradients. At the moment of failure or impact of lightning, fault currents should flow to the ground. The impulse characteristics might be used to determine the transient behaviour of grounding systems subjected to lightning discharge. Understanding these characteristics allows estimating the ground potential rise of the WTGS to examine the lightning performance of such systems. Several techniques should be considered for the conception of efficient grounding systems of the wind turbines, where the purpose is to decrease the step voltage, touch voltage, and the equivalent grounding impedance [4].

In the literature, the appropriate modelling of WTGS was the subject of many researchers (e.g., [5]–[7]). The main objective is to estimate the total wind farm ground impedance using different techniques. In addition, various geometric arrangements of WTGS have been selected to be experimentally or numerically studied. Indeed, many numerical models can be found in the literature, which have been developed to analyse the transient behaviour of grounding systems under lightning strikes including the circuit approach (e.g., [8]), the transmission line theory (e.g., [9]–[13]) and the electromagnetic field approach (e.g., [14]). Hybrid approaches have also been elaborated (e.g., [15]).

The wind turbine protection against lightning discharges is mainly covered by the IEC 61400-24 standard [3], where different tests have been described. The main purpose of these tests is to verify the performance of the WTGS against lightning currents and evaluate damages. The IEC 61400-24 suggests the interconnection of the WTGS through horizontal electrodes to achieve low steady state grounding resistance. The WTGS interconnection is discussed in other works, es- pecially for resistive soils (e.g., [16]–[18]). So also, the effect of interconnection on the lightning surge response of wind turbine grounding has been investigated (e.g., [13], [19], [20]).

In wind farm, turbines with rotating blades can have dynamic height, changing according to the position of the blade versus time. In moderate weather, multiple upward leaders can occur on tall objects by a close Cloud-to-Ground lightning strike [21]. In this case, the upward leaders attract the lightning and the discharge might be realised in random manner through the highest turbine. Better understanding of this phenomenon and its effect might be a key factor in the determination of thelightning performance of WTGS. Obviously, there is a need for more results that takes into consideration the influence of the injection point on the lightning response of WTGS in wind farm.

Based on the transmission line approach, this paper proses to discuss the transient response of isolated and

• *O. Kherif, S. Chiheb, M. Teguar and A. Mekhaldi are with Laboratoire de Recherche en Electrotechnique - Ecole Nationale Polytechnique (ENP), BP 182 El Harrach 16200 Algiers, Algeria.*
E-mail: omar.kherif@g.enp.edu.dz

Manuscript received December 17, 2017; revised March 2, 2018.

interconnected grounding systems of wind turbines. The results produced in time domain consisting on the transient potential evolution, where the influence of the soil parameters has been taken into account. Different magnitudes and frequencies of impulse currents have been also considered, related to the first and subsequent lightning strikes. In addition, the paper provides a means of estimating the temporal variations of the WTGS potential of interconnected system and the feed point effect have been investigated. The obtained results and discussions could be useful in the design of effective grounding systems,in wind farms.

2 Grounding Structure and Problem Description

2.1 Grounding System Structure

Fig. 1 depicts the considered WTGS, corresponding to a typical arrangement of wind turbines located in Kutubdia, onshore wind farm of Bangladesh [19]. This farm contains the total of 50 turbines, where the power of each wind turbine is about 20kW. The grounding system is constituted by a combination of two squared-shape grids reinforced by four vertical rods. This system is horizontally buried at 2m depth in uniform non-magnetic soil characterized by resistivity ρ_{soil} and relative permittivity ϵ_r . The inner grid has a side $L_1 = 6\text{m}$ and the second (outer) one has a side $L_2 = 12\text{m}$. The four rods of $H_R = 10\text{m}$ length are installed in the outer grid corner points. The same structure of grounding system has already been used by many researchers (e.g., [5], [20]).

In the interconnected WTGSs, two identical grounding systems or more are linearly arranged. The distance between two wind turbines is $D = 100\text{m}$. This later has been chosen according to the diameter of wind turbine blades; i.e., equal to or longer than three times the diameter of wind turbine blades as sated in [20]. Fig. 2 illustrates a small wind turbine farm contained three elementary circuits, corresponding to the studied system in this investigation.

Even, for the same grounding system configuration, the impedance value largely varies according to the position of the injection point on the grounding system [22]. Similarly to the WTGS, the location of feed point of the injected current might have a great influence on the transient characteristic of the interconnected WTGSs. Indeed, the analysis of the injection point effect (i.e., the wind turbine subjected to the lightning discharge current) on the transient response of grounding systems has been investigated for the three-interconnected wind turbines. For this case, the impulse current has been injected firstly to one of the WTGS situated at the extremities (i.e., on (A) or (C)), then on the wind turbine (B).

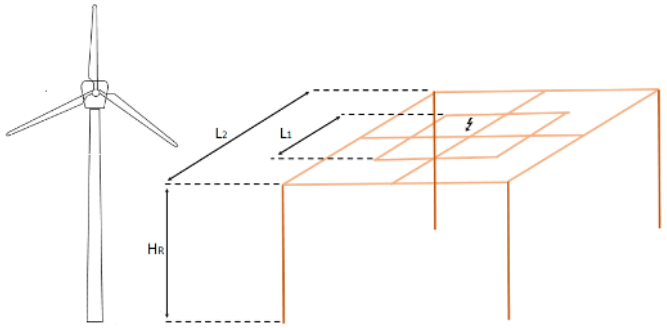

Fig. 1. Representation of a single WT and its grounding system.

2.2 Grounding System Model

The squared-shape grounding grids, selected here, are constituted from arrangements of vertical and horizontal ground electrodes. Basing on the transmission line approach, the system is divided into "N" number of elementary ground electrodes, of length l, arranged according to the global grounding grid structure. Thereafter, each elementary electrode forming the global system is subdivided into "n" number of segments. Now, each segment has a length $\Delta l = l/n$, which should be less than one tenth of the minimum wavelength of the highest frequency component of the injected current to ensure high accuracy [10]. The infinitesimally short segment improves the accuracy at the expense of the running time which increases significantly.

According to [10], $\Delta l = 10\text{cm}$ was found to be satisfactory. Each elementary ground electrode is then represented by a distributed parameter, lossy transmission line formed by cascading the conductor segments as shown in Fig. 3.

The transmission line approach method has been applied to systems of $r \ll 2l$ and $4h \ll l$, where r is the conductor radius and h is the burial depth. These conditions are satisfied in this investigation. Hereafter, each elementary electrode is studied separately taking into account the connection point between elementary electrodes. For the sake

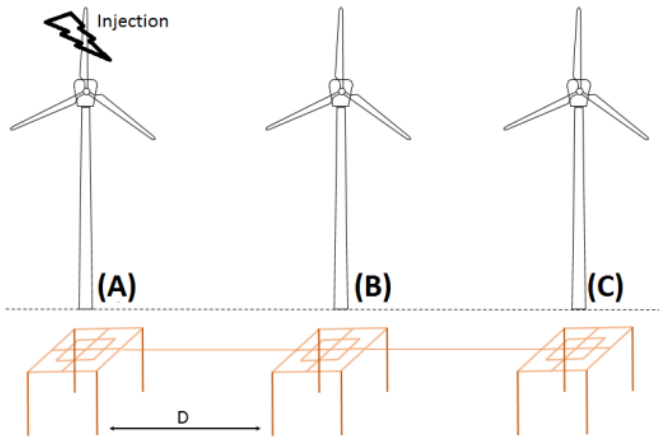

Fig. 2. Representation of a single WT and its grounding system.

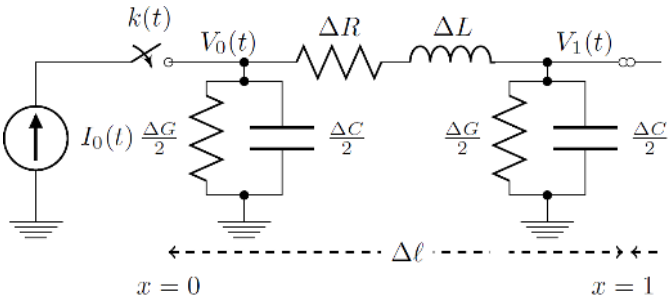

Fig. 3. Equivalent circuit of the each conductor segment of Δl length.

of simplicity of the general solution, the mutual coupling effects (inductive, capacitive and resistive) has been ignored in this investigation.

An impulse current exciting the elementary grounding conductor at its sending end generates travelling waves propagating along the conductor. The transient behaviour of each conductor segment can be governed by the following transmission line equations (i.e., the telegrapher's equations) [10]:

$$V(x_i,t) - V(x_{i+1},t) = \Delta R\ I(x_i,t) + \Delta L \frac{\partial I}{\partial t}(x_i,t) \quad (1)$$

$$I(x_i,t) - I(x_{i+1},t) = \Delta G\ V(x_i,t) + \Delta C \frac{\partial V}{\partial t}(x_i,t) \quad (2)$$

in which, ΔR, ΔL, ΔG, and ΔC are, respectively, the resistance, the inductance, the conductance, and the capacitance of ground conductor segment of Δl length.

The distributed parameters depend on the segment location, the dimension and the properties of the conductors as well as on the soil electrical characteristics. The series resistance of each segment of Δl length can be calculated as function of the conductor radius r and resistivity ρ cond. using Ohm's formula:

$$\Delta R = \frac{\rho_{cond.}\Delta l}{2\pi r^2} \quad (3)$$

Assuming that the current along the axis of the conductor segment is uniform and that the soil is non-magnetic material (its permeability $\mu = \mu_0$), the inductance ΔL can be calculated using Neumann's law, which states that:

$$\Delta L_{ij} = \frac{\mu_0}{4\pi}\left\{\int_{\Delta l_i}\int_{\Delta l_j}\frac{1}{r_{ij}}\vec{dl}_i\vec{dl}_j\right\} \quad (4)$$

Since the mutual components are neglected, the self-inductance of each conductor segment of Δl length and buried at h-depth can be calculated for horizontal and vertical electrode segments, respectively, as follows [10]:

$$\Delta L = \frac{\mu_0\Delta l}{4\pi}\left\{\log\left(\frac{l}{r}\right) + \log\left(\frac{l}{2h}\right)\right\} \quad (5)$$

$$\Delta L = \frac{\mu_0\Delta l}{4\pi}\left\{\log\left(\frac{4l}{r}\right) - 1\right\} \quad (6)$$

According to [10], the self-capacitance and the self-conductance of each conductor segment of Δl length could be calculated, respectively, by:

$$\Delta C = \frac{2\pi\,\epsilon_{soil}\,\Delta l}{\left\{\log\left(\frac{l}{r}\right) + \log\left(\frac{l}{2h}\right)\right\}} \quad (7)$$

$$\Delta G = \frac{2\pi\,\Delta l}{\rho_{soil}\left\{\log\left(\frac{l}{r}\right) + \log\left(\frac{l}{2h}\right)\right\}} \quad (8)$$

or horizontal electrodes as well as for vertical conductor segments using:

$$\Delta C = \frac{2\pi\,\epsilon_{soil}\,\Delta l}{\left\{\log\left(\frac{2l}{r}\right) - 1\right\}} \quad (9)$$

$$\Delta G = \frac{2\pi\,\Delta l}{\rho_{soil}\left\{\log\left(\frac{2l}{r}\right) - 1\right\}} \quad (10)$$

The unknown time dependent electrical quantities, $V_i(x_i,t)$ and $I_i(x_i,t)$, depend on the location "x_i" of the segment regarding the axis of the elementary conductor. The solution of the telegrapher's equations is performed iteratively in the modal domain, where a system of n coupled segments is represented by n independent single-phase lines (n segments) by means of a similarity transformation. The validation of the above model (TLM) is achieved, previously in [13], by performing comparison with the lightning response of isolated WTGS using NEC-4 (Numerical Electromagnetics Code) reported in [20]. The lightning response concerns the transient potential computed for a test current of $0.25/250\mu$s impulse shape.

3 Isolated WTGS Results

In order to study the transient behaviour of isolated WTGS, the system of Fig. 1 has been considered. Such systems are subjected to two lightning current waveforms, which are related to the first and subsequent strikes:

- The first strike lightning impulse current has a peak value $I_p = 30$kA, a rise time $T_1 = 5\mu$s, and an impulse duration $T_2 = 50\mu$s ;
- The subsequent strike current is characterized by 12kA peak value and $0.5/50\mu$s impulse shape.

The previous parameters of the injected currents, appropriately reproduce the observed concave of typical recorded lightning current impulses, used in various published works e.g., [23]–[25]). Therefore, these currents are reproduced by means of a usual double exponential time expression as follows [26]:

$$I(t) = I_0(\exp(-a\,t) - \exp(-b\,t)) \quad (11)$$

where,

$$\begin{cases} a = \frac{0.69}{T_2} \\ b = \frac{2.2}{T_2} \\ I_0 = \frac{I_p}{\left\{1+\left(\frac{a}{b}\right)\left(\log\left(\frac{a}{b}\right)\right)\right\}} \end{cases}$$

The transient ground potential rise is calculated at the center point of the modelled grounding system subjected to lightning impulse current shown in Fig. 4.

Clearly, the first current has a slow rise time with a high magnitude peak regarding the subsequent one, which is a fast rise time impulse with relatively a low magnitude peak.

3.1 Transient potential of WTGS

Fig. 5 shows examples traces of the WTGS ground potential rise (GPR) at the injection point obtained for soils with

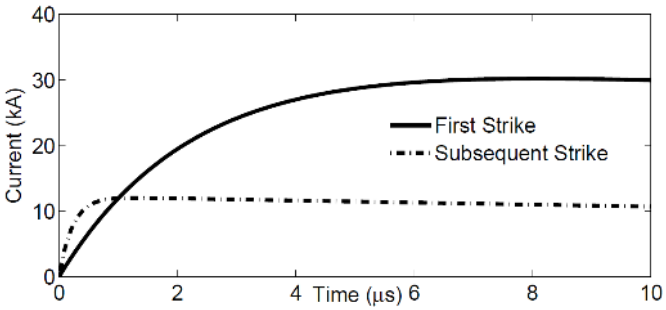

Fig. 4. Current waveform for the first and subsequent lightning strikes.

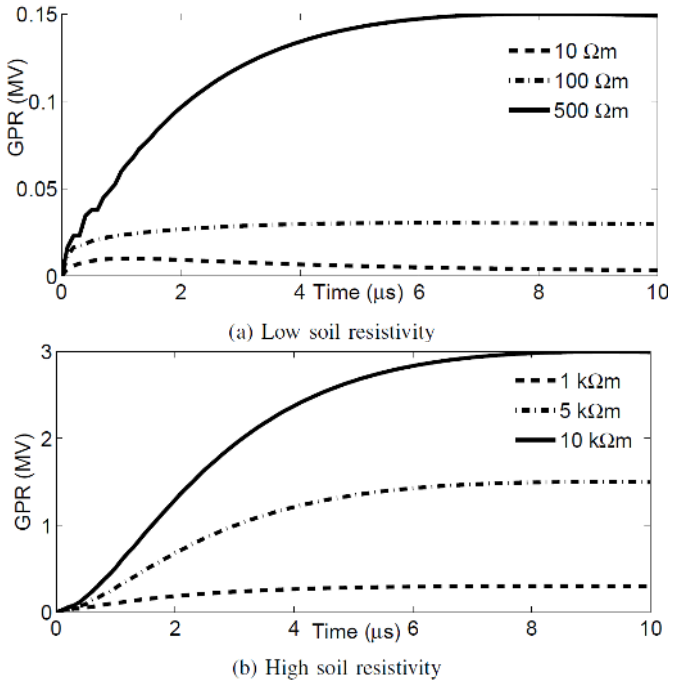

Fig. 5. GPR at the injected point of grounding system subjected to the first lightning strike for various resistivities.

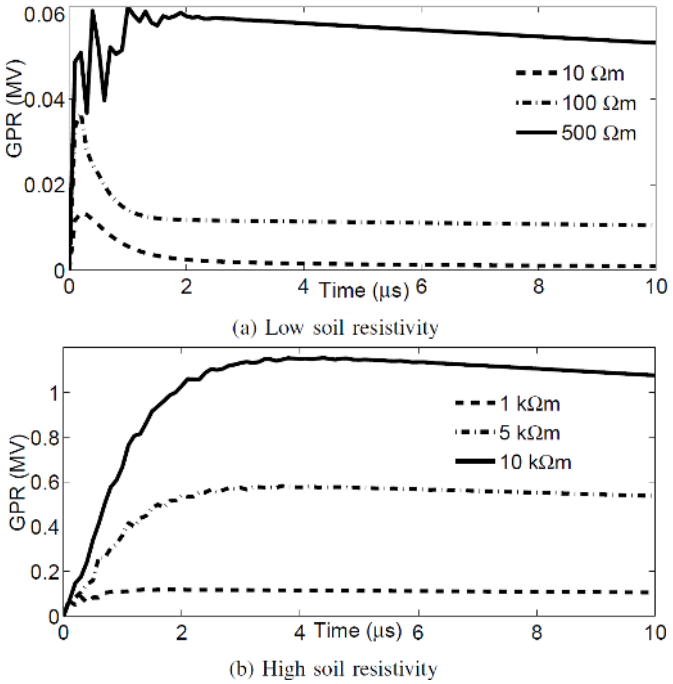

Fig. 6. GPR at the injected point of grounding system subjected to the subsequent strike current for various soil resistivities.

low resistivities of 10, 100, 500Ωm and high ones of 1, 5 and 10kΩm. The corresponding results in this figure are obtained for the first lightning strike injection.

From this figure, the soil resistivity has a significant influence on the transient response of WTGS. The lower the resistivity of the soil in Fig. 5a, the lower magnitude GPR is. Indeed, the increase in the resistivity of the ground as shown in Fig. 5b leads to an increase in the peak values of the current and potential waves.

Since the grounding impedance mostly depends on the front time of the injection current, the ground potential rise has been also computed for the subsequent lightning strike. The current waveform is characterized by a fast rise time regarding the first lightning strike current. Fig. 6 illustrates the results computed for different values of soil resistivity ranging between 10Ωm and 10kΩm. Figs. 6a and 6b show the WTGS ground potential rise computed for soil with low resistivities of 10, 100, 500Ωm and high ones of 1, 5 and 10kΩm, respectively. This figure shows that the current front time has an important influence on the transient response of WTGS. Considerable undulations appear following to the injection of this fast impulse current. This may be due to existence to the reactive (inductive-capacitive) effect while the current has a large gradient for the subsequent lightning strike.It should be emphasized that above characteristics are related to the fast transient period only, from the initial instant until the GPR curve reaches its peak. After that, in the slow transient period, the performance of the ground electrodes is characterized by low frequency grounding resistance.

3.2 Transient impedance of WTGS

For designing of any grounding system, the steady-state grounding resistance should be considered. Such resistance is computed for the case of low or industrial frequencies, in which the grounding system can be modelled as a resistance. However, the performance of grounding system at high frequency is different and it would be determined by the grounding impedance parameter, defined by the ratio potential on current [10]. Fig. 7 shows the time variation of the transient impedance during the first 10μs of application of the impulse current. The results correspond to soil with 10, 100, 500, 1k, 5k and 10kΩm resistivities and relative permittivity ranging between 80 and 10. For a given soil resistivity, the transient impedance falls abruptly from the same high initial surge value, reaches a minimum value, and increases before tending to a constant limit. The first phase corresponds to the rising wave front and describes the high-frequency behaviour of the grounding system. This phase lasts about 1μs, which slightly decreases with the increase of the soil resistivity. The second phase presents a progressive change, which might be associated with the low-frequency resistance of grounding system. It reflects the grounding system behaviour during the slow period corresponding to wave tail of the impulse current.

The steady-state grounding resistance of the modelled grounding system is about 30Ω computed for 500Ωm soil resistivity [20]. For soil resistivity value less than 500Ωm, the transient impedance is lower than that computed for the steady-state one (30Ω). In this case, there is no risk for the wind turbine system since the low impedance facilitates the flow the fault current into the ground. For high values of soil resistivity (1kΩm and more), the transient impedance is higher than the steady-state one due to inductive behaviour of the grounding system. Such findings are more significant as the resistivity of soil becomes important. It is worth noting that the same ascertainments are found for the subsequent strike.

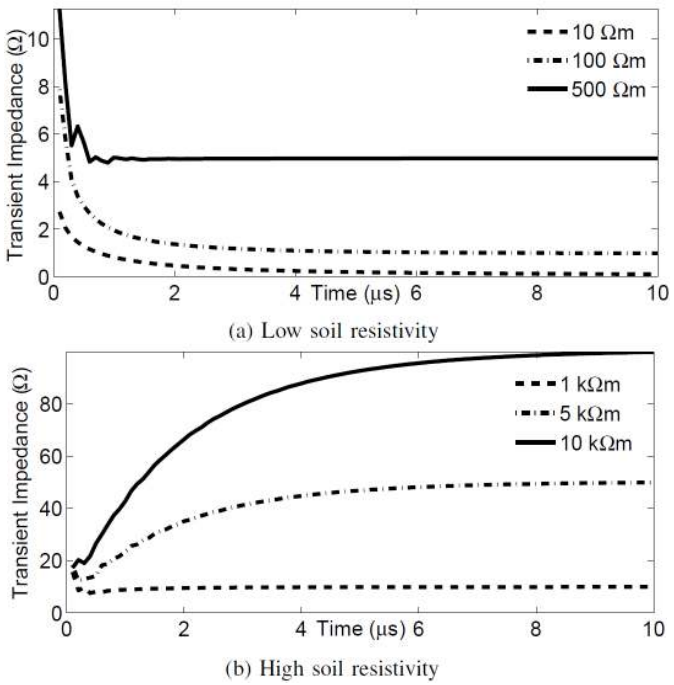

Fig. 7. GPR at the injected point of grounding system for various resistivities.

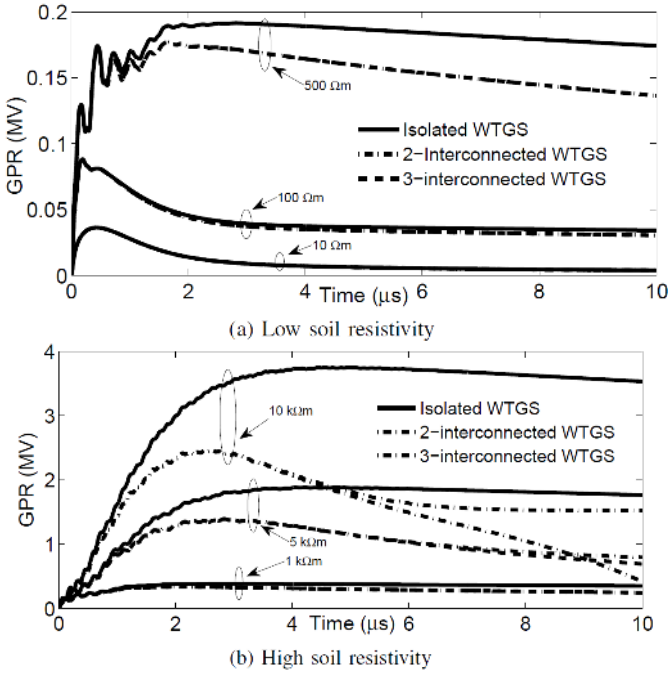

Fig. 8. GPR at the injected point of grounding system for various resistivities.

4 Interconnection Effect

In this section, we have interested to study the WTGS interconnection effect on the transient response of grounding system in wind farm. Such grounding system has been buried in soil with different resistivities ranging between $10\Omega\mathrm{m}$ and $10\mathrm{k}\Omega\mathrm{m}$. An impulse current, with a standard waveform [27], of $1.2/50\mu\mathrm{s}$ impulse shape and $50\mathrm{kA}$ peak has been adopted as the injected current into the grounding system. Identical WTGSs have been selected to be interconnected (placed end to end as shown in Fig. 2) by horizontal electrodes of $100\mathrm{m}$ long.

Fig. 8 shows the obtained results consisting in the transient response at the feed point associated to isolated, two and three interconnected WTGS. The results of the isolated WTGS serve as reference of comparison. Figs. 8a and 8b are, respectively, related to the results computed for low and high values of soil resistivity.

From Fig. 8, the potential magnitudes increase with the soil resistivity; the higher the value of soil resistivity, the greater the magnitude of the potential peak. In addition, undulations have been observed in the case of soil resistivity superior or equal to $500\Omega\mathrm{m}$. However, the potential waves are damped faster in the soil resistivity inferior to $500\Omega\mathrm{m}$ in Fig. 8a.

Generally, the transient potential magnitude decreases with the increase of the number of elementary circuits of grounding system. In fact, the transient potential magnitude is higher inthe isolated WTGS than in interconnected ones. This decrease is slight in the case of low soil (10 and $500\Omega\mathrm{m}$) as shown in Fig. 8a and visible elsewhere (resistivities between 1 and $10\mathrm{k}\Omega\mathrm{m}$) as illustrated in Fig. 8b. For instance, the reduction in both interconnected systems is up to 25% for $500\Omega\mathrm{m}$ soil resistivity against 75% and 81% for the highest value of soil resistivity for two and three interconnected WTGS, respectively. This implies that the dissipation of the current in the low soil resistivity is rather carried out using only a single circuit of grounding system (isolated WTGS) where the lightning current is injected. The interconnection is not very effective to reduce the maximum voltage rise of grounding system for low soil resistivities.

5 Injection Point Effect

A small wind farm of three-interconnected WTGS has been selected. Such system has been buried in soil with different resistivities ranging between $10\Omega\mathrm{m}$ and $10\mathrm{k}\Omega\mathrm{m}$. The injected current is characterized by $1.2/50\mu\mathrm{s}$ impulse shape and $50\mathrm{kA}$ peak, corresponding to a standard waveform [27].

This impulse current is injected on only one of the three interconnected WTGS. Fig. 9 shows the transient response of the studied system concerning the GRP at the feed point. The characteristics show the obtained results for several soil resistivities; Figs. 9a and 9b correspond to low and high soil resistivity values, respectively.

From Fig. 9, the GPR is decreased and the dissipation of the current becomes practically faster for the injection at WT-B comparing to the obtained results for the injection in the extensibility. The gap between them increases with the soil resistivity. A considerable decrease in the amplitude reaches the order of 25% for $500\Omega\mathrm{m}$ soil resistivity and up to60% for very high soil resistivity. Moreover, for $10\mathrm{k}\Omega\mathrm{m}$ soil resistivity, oscillations appear. They might be imputed to the reflection of the current signal Indeed, the current cannot be dispersed easily during the propagation. Similar oscillations were observed by [28] when the soil conductivity is poor.

6 Discussion

The use of grounding systems of various geometries and arrangements is essential to ensure the safety of people

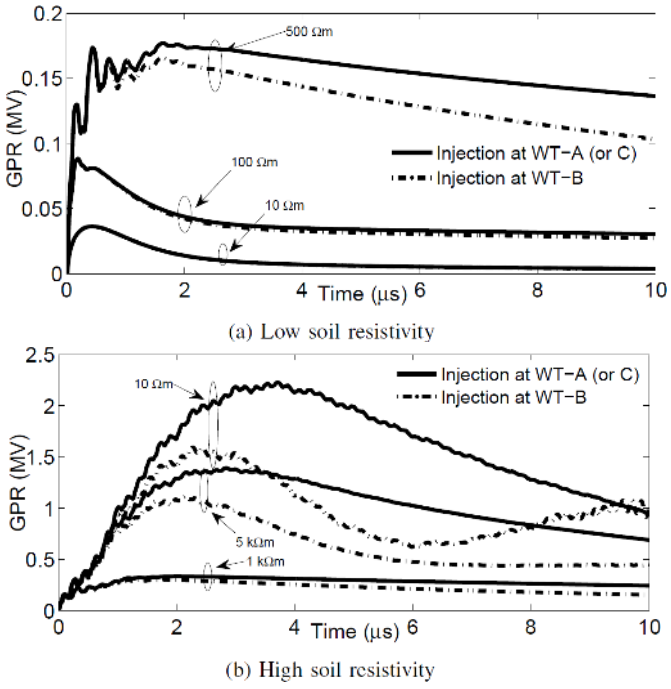

Fig. 9. GPR at different injected point of three-interconnected WTPGS for various soil resistivities.

and equipment. The grounding systems are designed to provide a low impedance path for fault or transient currents flowing into the ground. The steady-state grounding resistance should be considered for designing of any grounding system in industrial or low-frequency applications. However, under transient high frequency and impulse currents, the response of grounding systems is significantly different from that under steady state low frequency currents. The reason is that, under transient conditions, their behaviour is affected by numerous factors such as the magnitude and the shape of the impulse current as well as the soil electrical parameters.

In the present investigation, the transient behaviour of typical wind turbine grounding system has been analysed using the transmission line theory. The influence of the soil resistivity, ranging from $10\Omega\mathrm{m}$ to $10\mathrm{k}\Omega\mathrm{m}$, on transient behaviour was examined for isolated WTGS. The results show that the soil resistivity has a significant influence on the transient response of WTGS. The lower the resistivity of the soil, the lower the GPR magnitude. Since the grounding impedance mostly depends on the front time of injection current, the GPR has been computed for the subsequent lightning strike. Such current waveform is characterized by a fast rise time regarding the first lightning strike current. The results show an important influence on the transient response of WTGS due to the fast rise time impulse current. This later causes considerable undulations on the GPR waveform regarding those computed for the first strike. This may be due to the inductive effect, which appears while the lightning current has a large gradient.

In addition, the increase in the resistivity of the ground leads to an increase in the peak values of the potential waves for both first and subsequent lightning impulse currents Such high-magnitudes of GPR could be the probable cause of the malfunctions of the electrical and/or control systems inside wind turbines. This finding is very important, especially, when grounding systems of the wind turbines are installed in rocky terrain. To achieve better transient response with low magnitude of GPR, certain number of additional electrodes should be added, reinforcing the actual grounding system. Such proposition has been already reported in the literature (e.g., [19], [20]). The interconnection between WTGS in wind farm, object of this section, is a practice among others to reinforce the grounding systems. Such interconnection is beneficial to reduce the GPR peak when lightning current hits a wind turbine.

In this work, a small wind farm of three-interconnected WTGS has been selected to study the influence of the injection point on the transient response of interconnected WTGS. The impulse current has been adopted to be injected on only one of the three-interconnected WTGS. The GPR magnitude is decreased for the injection at the middle wind turbine (B) for which the current dissipation is more faster compared to GPR obtained for the injection at the WT located at the extremity. The gap between them increases with the soil resistivity, which implies that the difference is accentuated when the groundingsystem is installed at the soil of the highest resistivity. Such findings are an indicator that might be helpful in improving the lightning protection system in wind farm. It is also a useful to introduce some practical criteria for engineering applications to design ground systems against lightning. It is recommended that the wind turbines of the middle should be more taller than the other, especially for those installed in areas with high value of soil resistivity.

7 Conclusion

The transient response of WTGS in wind farm has been analysed and the effect of the soil electrical resistivity has been studied. For isolated WTGS, the results show that the soil resistivity is a very influential factor in the transient response of grounding system. The increase in the soil resistivity leads to increase of the potential peak accompanied by some fluctuations. To minimise the potential magnitude and further dissipate the current, the interconnection is recommended for high resistive soils. The results show that the interconnection of WTGS leads to a decrease of the system impedance and facilitates the flow of the current into the ground. The feed point effect on the transient response of grounding system has been also discussed for a typical small wind farm. The results show that a low GPR magnitude has been obtained for the injection at the middle wind turbine. Indeed, it is suggested that the wind turbines of the middle should be more taller than the other, especially for those installed in areas with high values of soil resistivity. The results would be helpful to accurate lightning protection in wind farms.

References

[1] A. A. Razi-Kazemi and A. RajabiNezhad. Protection of wind electrical power energy systems against indirect lightning strike surge. In *2016 24th Iranian Conference on Electrical Engineering (ICEE)*, pages 1388–1393, May 2016.

[2] N. D. Hatziargyriou, M. I. Lorentzou, I. Cotton, and N. Jenkins. Transferred overvoltages by windfarm grounding systems. In *8th International Conference on Harmonics and Quality of Power. Proceedings (Cat. No.98EX227)*, volume 1, pages 342–347 vol.1, October 1998.

[3] TR IEC. 61400-24 "Wind turbine generator systems–Part 24: Lightning protection". *IEC: Switzerland*, 7, 2002.

[4] K. Yamamoto, S. Yanagawa, K. Yamabuki, S. Sekioka, and S. Yokoyama. Analytical Surveys of Transient and Frequency-Dependent Grounding Characteristics of a Wind Turbine Generator System on the Basis of Field Tests. *IEEE Transactions on Power Delivery*, 25(4):3035–3043, October 2010.

[5] B. Nekhoul, B. Harrat, L. Boufenneche, M. Chouki, D. Poljak, and K. Kerroum. A simplified apporoach to the study of electromagnetic transients generated by lightning stroke in power network. In *2014 International Symposium on Electromagnetic Compatibility*, pages 595–600, September 2014.

[6] M. E. M. Rizk, F. Mahmood, M. Lehtonen, E. A. Badran, and M. H. Abdel-Rahman. Investigation of Lightning Electromagnetic Fields on Underground Cables in Wind Farms. *IEEE Transactions on Electromagnetic Compatibility*, 58(1):143–152, February 2016.

[7] N. Jenkins and A. Vaudin. Earthing of Wind Farms. *Wind Engineering*, 18(1):37–43, 1994.

[8] R. Rüdenberg. *Electrical shock waves in power systems: traveling waves in lumped and distributed circuit elements*. Harvard Univ Pr, 1968.

[9] E. D. Sunde. *Earth conduction effects in transmission systems*. Dover Publications Inc., 1949.

[10] O. Kherif, S. Chiheb, M. Teguar, A. Mekhaldi, and N. Harid. Time-Domain Modeling of Grounding Systems' Impulse Response Incorporating Nonlinear and Frequency-Dependent Aspects. *IEEE Transactions on Electromagnetic Compatibility*, 60(4):907–916, August 2018.

[11] S. Chiheb, O. Kherif, M. Teguar, A. Mekhaldi, and N. Harid. Transient behaviour of grounding electrodes in uniform and in vertically stratified soil using state space representation. *IET Science, Measurement & Technology*, January 2018.

[12] L. Grcev and M. Popov. On high-frequency circuit equivalents of a vertical ground rod. *IEEE Transactions on Power Delivery*, 20(2):1598–1603, April 2005.

[13] O. Kherif, S. Chiheb, M. Teguar, and A. Mekhaldi. On the analysis of lightning response of interconnected wind turbine grounding systems. In *2017 5th International Conference on Electrical Engineering - Boumerdes (ICEE-B)*, pages 1–4, October 2017.

[14] L. Grcev and F. Dawalibi. An electromagnetic model for transients in grounding systems. *IEEE Transactions on Power Delivery*, 5(4):1773–1781, October 1990.

[15] R. Andolfato, L. Bernardi, and L. Fellin. Aerial and grounding system analysis by the shifting complex images method. *IEEE Transactions on Power Delivery*, 15(3):1001–1009, July 2000.

[16] M. I. Lorentzou, N. D. Hatziargyriou, and B. C. Papadias. Analysis of wind turbine grounding systems. In *2000 10th Mediterranean Electrotechnical Conference. Information Technology and Electrotechnology for the Mediterranean Countries. Proceedings. MeleCon 2000 (Cat. No.00CH37099)*, volume 3, pages 936–939 vol.3, May 2000.

[17] V. T. Kontargyri, I. F. Gonos, and I. A. Stathopulos. Frequency response of grounding system of wind turbine generators. *A A*, 3(1):1, 2005.

[18] B. Hermoso. Wind farm earthing installations: rated and lightning frequencies behaviour. In *Proceedings of International Conference on Grounding and Earthing (GROUND'2006)*, pages 411–414, 2006.

[19] M. R. Ahmed. Analytical studies of lightning over-voltages grounding system of small wind turbine. In *2014 9th International Forum on Strategic Technology (IFOST)*, pages 373–377, October 2014.

[20] M. R. Ahmed and M. Ishii. Electromagnetic analysis of lightning surge response of interconnected wind turbine grounding system. In *2011 International Symposium on Lightning Protection*, pages 226–231, October 2011.

[21] A. C. Garolera, K. L. Cummins, S. F. Madsen, J. Holboell, and J. D. Myers. Multiple Lightning Discharges in Wind Turbines Associated With Nearby Cloud-to-Ground Lightning. *IEEE Transactions on Sustainable Energy*, 6(2):526–533, April 2015.

[22] S. Visacro. A Comprehensive Approach to the Grounding Response to Lightning Currents. *IEEE Transactions on Power Delivery*, 22(1):381–386, January 2007.

[23] L. Grcev. Modeling of Grounding Electrodes Under Lightning Currents. *IEEE Transactions on Electromagnetic Compatibility*, 51(3):559–571, August 2009.

[24] F. Rachidi, W. Janischewskyj, A. M. Hussein, C. A. Nucci, S. Guerrieri, B. Kordi, and Jen-Shih Chang. Current and electromagnetic field associated with lightning-return strokes to tall towers. *IEEE Transactions on Electromagnetic Compatibility*, 43(3):356–367, August 2001.

[25] D. Cavka, N. Mora, and F. Rachidi. A Comparison of Frequency-Dependent Soil Models: Application to the Analysis of Grounding Systems. *IEEE Transactions on Electromagnetic Compatibility*, 56(1):177–187, February 2014.

[26] M. W-Wik. Double exponential models for comparison of lightning, nuclear and electrostatic discharge spectra. In *Proc. 6th Symp. Tech. Exhib. Electromagn. Compat.*, volume 31F4, pages 169–174, Zurich, 1985.

[27] J. He and B. Zhang. Progress in Lightning Impulse Characteristics of Grounding Electrodes With Soil Ionization. *IEEE Transactions on Industry Applications*, 51(6):4924–4933, November 2015.

[28] N. Theethayi, V. A. Rakov, and R. Thottappillil. Responses of Airport Runway Lighting System to Direct Lightning Strikes: Comparisons of TLM Predictions With Experimental Data. *IEEE Transactions on Electromagnetic Compatibility*, 50(3):660–668, August 2008.